大阪
inter.noise 2011
Osaka Japan September 4-7

Large Eddy Simulation to Extract Fourth Order Space Time Turbulence Correlations in Jets including Microjet Injection

G.J. Page[1], M.E. Rife[2] and C.D. Pokora[3]

Aeronautical & Automotive Engineering, Loughborough University,

Leicestershire, LE11 3TU. UK

ABSTRACT

Jet noise is still a major component of overall aircraft noise emission at take-off, and its reduction is important to sustain the continuing growth of air transport. Computationally expensive Large Eddy Simulations can be used to assess the four-order spatio-temporal correlations so as to provide input and guidance to cheaper jet noise models. Large Eddy Simulations are presented for an isothermal Mach 0.75 jet at a Reynolds number of 1 million with and without microjet injection. The imposition of a numerical boundary layer trip inside the jet nozzle ensures that the shear layer is fully turbulent immediately downstream of the nozzle lip. The eight high-pressure microjets penetrate the shear layer producing streamwise vorticity on the inside of the jet. This dissipates before the end of the potential core and there is no effect on potential core length. The peak turbulence intensity within the shear layer is reduced, with the greatest reduction at locations aligned with the microjet injection points. The shapes of the fourth order correlation envelopes are little changed by the microjets, but there is a significant difference in the absolute magnitudes. Compared to a clean jet all significant correlation terms are reduced, with the reduction still occurring at x/D_j=6.5 where the effect of the microjets on the mean flow has dissipated. This reduction could be used to calibrate a jet noise model in order to take account of the microjets.

Keywords: Jet Noise, Large Eddy Simulation, Microjet

1. INTRODUCTION

Increasingly stricter international aircraft noise regulations and growing pressure from communities near airports are creating a requirement for quieter aircraft. With jet noise being a dominant contributing source of overall aircraft noise during take-off, a significant amount of work has focused on jet noise reduction. One method of noise reduction is the use of chevrons, or serrations, at the nozzle exit. These devices have been shown to reduce low frequency noise [1-3] and are gradually being introduced to aircraft, such as the Boeing 787 Dreamliner. A similar method of noise reduction is the addition of multiple small jets ('microjets') near the nozzle exit and directed into the main jet flow. The interaction creates pairs of counter-rotating axial vortices on the high-speed side of the jet shear layer and a reduction of low frequency noise, with minimal high frequency lift [1-2,4]. Microjets have an advantage over static devices such as chevrons in that they can be disabled when noise reduction is not necessary, such as cruise, thus eliminating fuel burn penalties during the majority of the mission.

Numerical simulations of microjets remain limited, with only a few published examples [5-8]. Huet et al.[6] performed a study of continuous and pulsed microjets on hot and cold jets. The Reynolds numbers of the main jet in the isothermal and hot simulations were $1x10^6$ and $3.2x10^5$,

[1] G.J.Page@lboro.ac.uk
[2] M.E.Rife@lboro.ac.uk
[3] C.D.Pokora@lboro.ac.uk

respectively. The simulation technique used by Huet et al. was the Monotonically Integrated Large Eddy Simulation (MILES) approach, in which no subgrid model is used. In their simulations, they used 12 microjets, with the inflow boundary conditions for each microjet being applied to one hexahedral cell.

The acoustic results of Huet et al. overpredicted the baseline round nozzle noise by about 6 dB. However, the noise reduction caused by continuous microjets was found to be about 1.5 dB for sideline noise, which agrees well with experimental results. It is possible that the discrepancy in the acoustic predictions is the result of the MILES approach and the noise reduction found in their simulations is due to the microjets shifting part of the noise spectrum to higher frequencies, which are unable to be properly resolved by an excessively coarse grid coupled with the MILES scheme.

Lew, Najafiyazdi, and Mongeau [7] employed a Lattice-Boltzmann Methodology LES (LBM-LES). The simulation was run at a Reynolds number of $1x10^5$ with 18 microjets surrounding the nozzle. Grid refinement in the region of the microjets resulted in 20 cells across each microjet, significantly finer resolution than Huet et al. As a result of using LBM-LES, the jet plume in their simulation has a distinct non-circular shape in both the clean nozzle and microjet simulations. Acoustically, the results from Lew et al.'s simulations show good agreement with experimental results. The simulation overpredicts the clean nozzle noise by 1 dB for observer angles lower than 80°. However, it does accurately predict a reduction in noise of about 1.5 dB, a similar result to that found in experiments of Alkislar [1] and Castelain [4].

Recently, Liu et al. [8] simulated an under-expanded nozzle with 12 microjets injecting into the supersonic jet. Their results captured the longitudinal vortices caused by the penetrating flow from the microjets. When the mass flow ratio between the microjets and main jet was increased the size and strength of these vortices increased, as did the thickness of the shear layer. Noise reductions were in agreement with experimental results, with near-field high frequency noise being increased.

The aim of the present work is to perform numerical simulations of a high subsonic jet fitted with eight microjets for comparison to an equivalent clean jet in order to assess the impact on the jet noise sources. The microjet parameters are based on the experimental work of Alkislar et al. [2].

This paper begins with a description of the computational method, grid and numerical parameters used in the simulations. Mean flow results are compared with experimental clean jet data and the clean and microjet simulations. Finally, spatio-temporal correlation data are presented to show the influence of the microjets.

2. Methodology

2.1 Solver

The computational solver is a finite volume pressure-based method using a multiblock structured grid. Whilst pressure-based solvers are typically used for low speed incompressible flows, the method has been extended to include compressibility with conservative state variables and can efficiently compute high speed flows including shock waves. The spatial discretization is a high order upwind scheme (equivalent to QUICK) and for LES the limiter is disabled. A four-stage Runge-Kutta scheme is available for temporal discretization, but with the small time-steps used in LES it has been found that a single stage backward Euler method is more efficient and has no impact on accuracy. The semi-implicit spatial discretization and the backward Euler temporal discretization allow larger time steps than typically required for stability by explicit density based methods.

2.2 Grid

Simulations were performed on a cylindrical grid with 438x102x360 (axial x radial x azimuthal) elements. This results in 15.1 million hexahedral elements over 11 blocks. The mesh extends $30D_j$ downstream, $10D_j$ in the radial direction, and $6D_j$ upstream of the nozzle exit to include the nozzle geometry for increased accuracy of flow development. Figure 1 shows *half* of the cylindrical computational domain, clearly indicating the nodal bunching in the regions of the nozzle exit and shear layer. The grid geometry is based on the JEAN experimental nozzle [14] and was originally used for clean jet simulations. At the nozzle lip the spacing is $0.0045D_j$, $0.004D_j$ and $0.0087D_j$ in the axial, radial and azimuthal directions. Note that the azimuthal spacing is approximately twice that of the axial and radial spacing at this key location, and approximately 720 azimuthal points would be need to achieve an ideal aspect ratio of unity. Grid-stretching is employed in each direction away from this region as the size of largest resolved structures increases downstream in the jet.

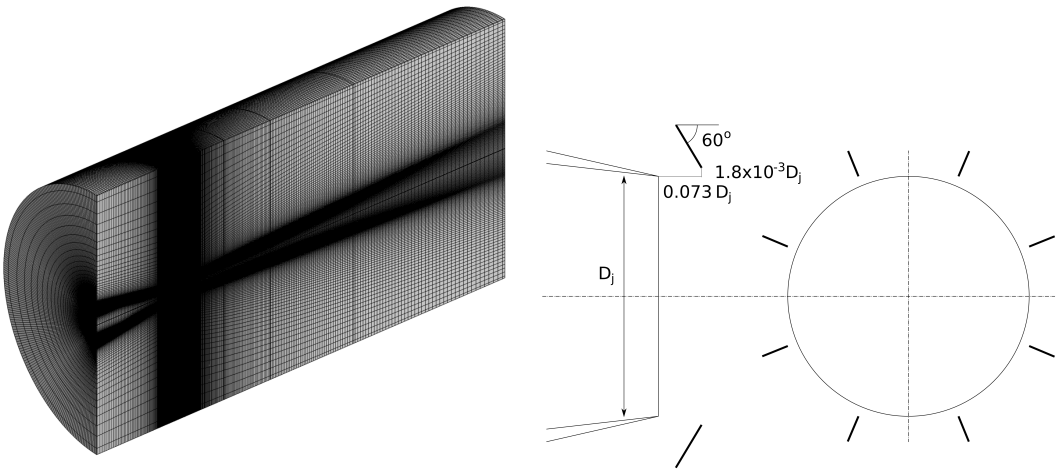

Figure 1: Computational grid and microjet nozzle configuration.

2.3 Nozzle Numerical Trip

The numerical trip is analogous to that often used in experimental work at moderate Reynolds number to avoid re-laminarisation in the favourable pressure gradient created by the nozzle contraction. The trip is applied by perturbing, at each computational time step, the flow solution in a ring of computational cells *within* the flow domain near the wall. At each point a random velocity perturbation is computed having a Gaussian distribution with a given turbulence intensity. This is then applied to a nine-point stencil around the given point in the structured grid. As this perturbation is applied sequentially across the cells in the plane, each cell will be updated nine times, and there will be a spatial correlation of the net perturbation between adjacent cells. However, the imposed perturbation has no temporal correlation. Figure 2 shows an isosurface of instantaneous vorticity with the trip visible on the left, the disturbances propagate through the convergent nozzle and then rapidly grow in the free shear layer.

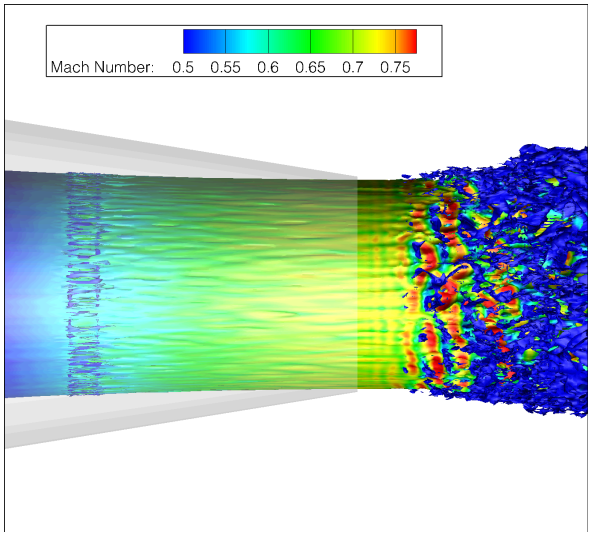

Figure 2: Isosurface of instantaneous vorticity coloured by Mach number, trip location and influence.

2.4 Microjet Configuration

Using the results of the clean jet simulation as a starting point, eight equally spaced microjets located just downstream of the nozzle exit were added to the simulation as shown in Figure 1. The microjets are equally spaced around the circumference of the jet nozzle and are located $0.073D_j$ downstream from the exit plane and $1.8\text{x}10^{-3}$ D_j radially outwards from the lip line. As a result of using an existing grid, the microjet resolution is restricted to 2x2 at their inlet, giving the microjets

an equivalent diameter of $D_{mj} = 0.021D_j$. The microjets were introduced to the simulation as pressure inlets located within the solution domain. Using this approach, the complex geometry associated with the microjet feed pipes around the nozzle is avoided. Furthermore, the inclusion of microjets in the simulation does not noticeably increase run time compared to the clean jet. The location of the microjets is such that the non-dimensional location is equivalent to Alkislar et al. [2]. The microjets are similarly inclined to the main jet axis by 60 degrees and they have a fully expanded Mach number of 1.19. The Reynolds number of the main jet and microjets are 1.3 million and 40,000 respectively (based upon jet velocity and diameter). The ratio of mass flow of each individual microjet to the main jet is 0.6×10^{-3}.

2.5 Miscellaneous

The Smagorinsky constant was set to 0.12 in both calculations; previous calculations had shown little sensitivity to this choice of constant. The radial and downstream boundaries have a freestream pressure boundary condition, whilst to assist with computational stability, a small co-flow velocity of $0.05U_j$ is added to the upstream boundary. The computations were initially run for approximately 120,000 time steps to achieve a statistically stationary flow-field, then filtered sub-samples of the entire flow were computed over 40 time step intervals for a further 80,000 time steps.

2.6 Two Point Spatio-Temporal Correlations

Through direct rearrangement of the Navier-Stokes equations, Lighthill's acoustic analogy provides a means of treating a turbulent flow as a distribution of quadrupoles [9].

Karabasov et al. [10] showed the important relationship between the Lighthill stress tensor, T_{ij} and two-point, two-time correlations $R_{ij,kl}$. An acoustic analogy based on information from these correlations has been shown to provide accurate results, when compared to experiments. Thus, a knowledge of how microjets affect the correlations may provide a means of modifying the jet noise model to take into account the microjets. The definitions of the two-point, two-time correlations used in this work have been defined previously [11-13].

It has been noted by Karabasov et al. that of the 21 unique fourth order correlations only six have significant amplitude to be necessary for inclusion in an acoustic source description, those correlation functions being R_{1111}, R_{1112}, R_{1212}, R_{1313}, R_{2222} and R_{3333}.

3. Results

Figure 3 shows an instantaneous isosurface of Mach number for the clean tripped and microjet cases. For both cases the flow leaving the nozzle rapidly develops into three-dimensional turbulence within $0.5D_j$; there is no evidence of laminar-like azimuthal vortex ring structures that often occur in large eddy simulations. The microjets can be seen to penetrate the jet shear layer, but further downstream they have no visible effect in this instantaneous picture. Successive slices of the mean Mach number are shown in Figure 4. After penetrating the jet shear layer, the microjets have the curious behavior that they distort the circular jet shear layer into an octagonal shape with planar sections between the microjets. At $x/D_j = 1$, the microjets have produced streamwise vorticity within the jet and this decays away so that by $x/D_j = 5$ the jet is essentially circular.

A comparison with some experimental data is shown in Figure 5; excellent agreement is found for the RMS fluctuations of axial velocity component in the shear layer and the jet potential core length which is unaffected by the presence of the microjets.

Looking in detail at radial profiles of turbulence kinetic energy in the jet shear layer (Figure 6), the microjets create a small reduction in peak turbulence kinetic energy including at the last station where the microjets have mixed out. It perhaps would have been expected that the introduction of the high pressure ratio microjets would increase levels of unsteadiness and so increase turbulence kinetic energy.

Detailed measurements of turbulent correlations are rare and so to indicate the fidelity of the current simulations, comparisons are made in Figure 7 against experimental data from Pokora [12]. It should be noted that the experiments used a PIV measurement technique in a low speed water rig at a Reynolds number of 4×10^4. The good agreement between simulation and experiment is an indication that the turbulence in a jet shear layer can be characterized in a universal manner relatively independent of Reynolds number and Mach number.

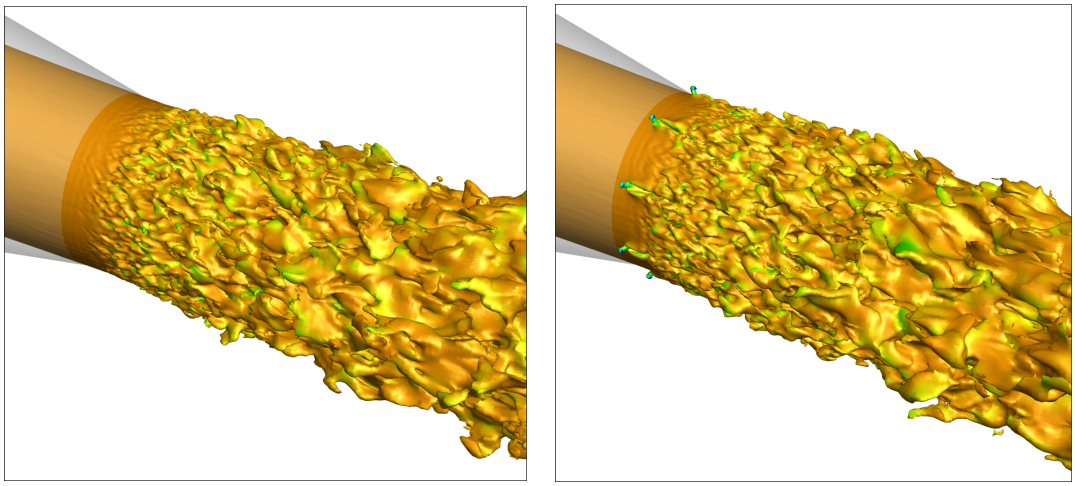

a) clean tripped b) microjet

Figure 3: Instantaneous Mach=0.4 isosurface, coloured by axial velocity.

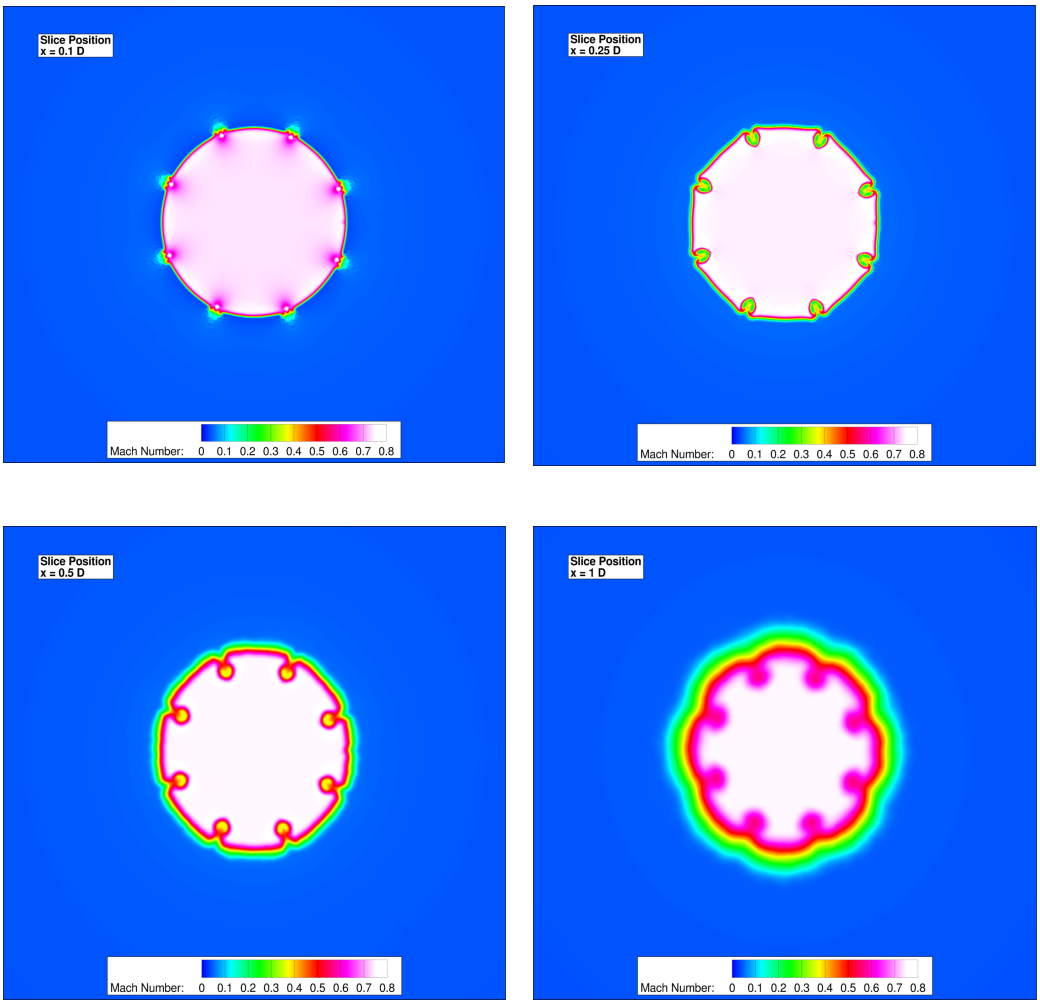

Figure 4: Contours of mean Mach number for initial jet development with microjets.

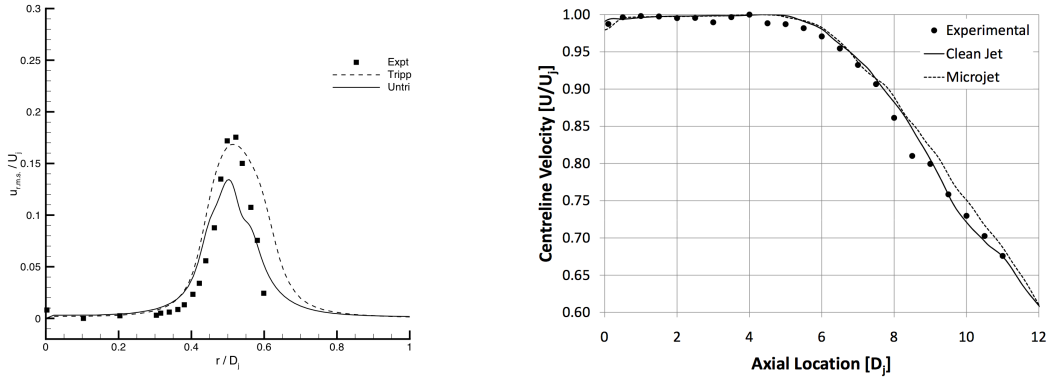

a) axial RMS velocity fluctuations profile at x/D_j=1.0 b) axial mean velocity along jet centerline

Figure 5: Mean flow comparison with experiment [14].

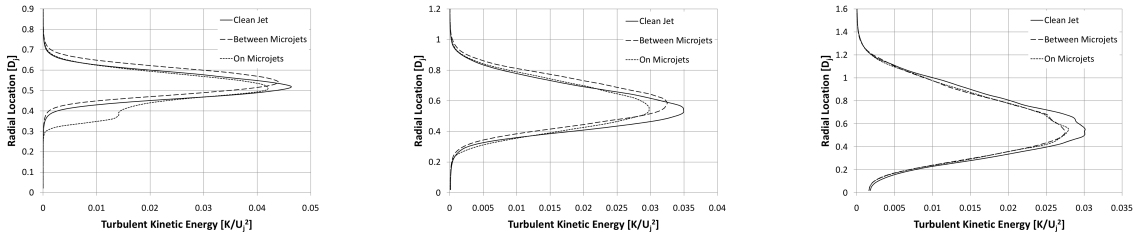

a) x/D_j=1.0 b) x/D_j=2.5 c) x/D_j=5.0

Figure 6: Radial turbulence profiles, clean jet and microjet case.

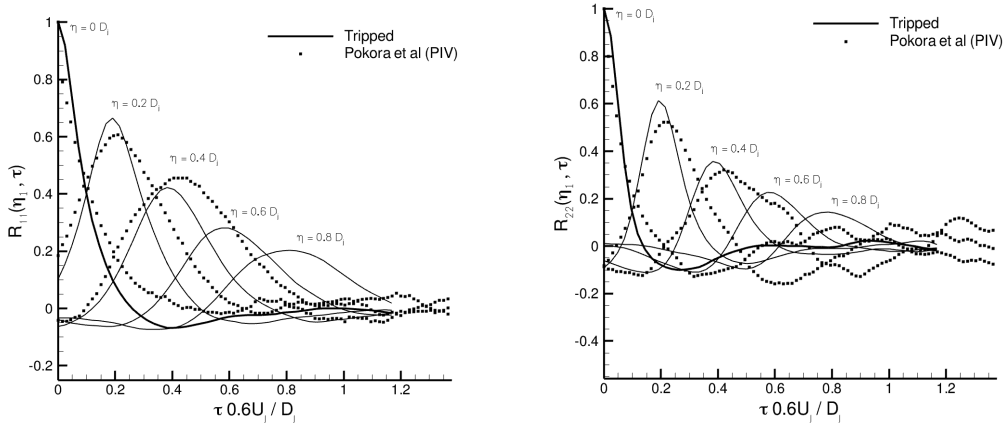

a) R_{11} b) R_{22}

Figure 7: Second order correlation, clean tripped jet, lipline, x/D_j=1.5, comparison with experiment [12].

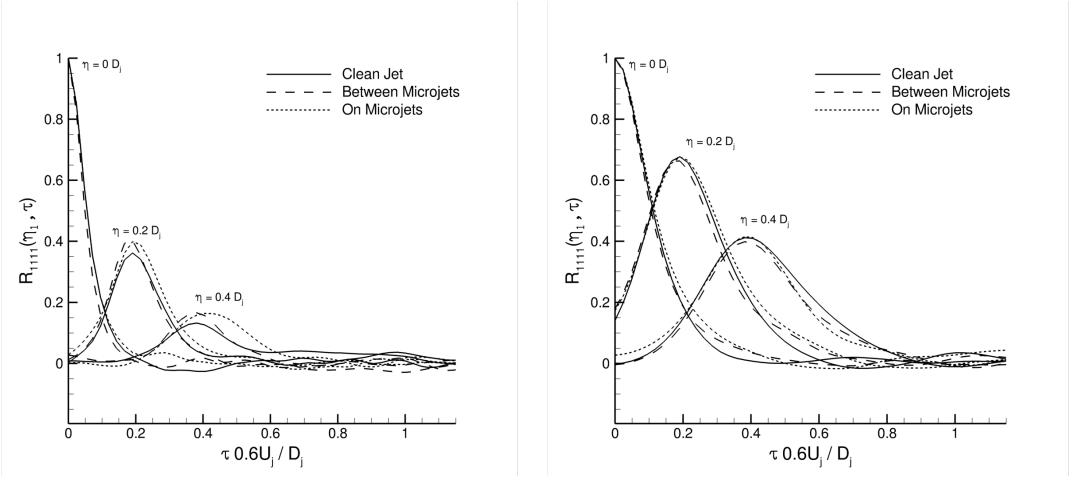

a) x/D_j=1.5 b) x/D_j=4

Figure 8: Fourth order correlation R_{1111}, microjet and clean tripped jet, lipline.

Of interest for jet noise modelling are the fourth order correlations, which can be used to determine noise sources. Figure 8 shows the axial lipline R_{1111} correlation envelopes for two stations. At the early station close to the microjet, the higher microjet peaks show a small increase in correlation that would be consistent with turbulent structures generated from the microjet. At the further downstream station the correlations are very similar, again indicating a universality of this correlation characterization. This is relevant to jet noise modeling in that the models used to recover this envelope need not be modified to account for microjets.

However, the normalization of these envelopes hides the potential differences in absolute magnitude of the correlations. Figure 9 shows the magnitudes of selected important correlation components, normalized by R_{1111} of the clean jet case. At almost all stations and components the presence of the microjets reduces the magnitude of the correlations. The largest reduction occurs in the azimuthal R_{3333} term, which perhaps indicates how the streamwise vortical microjet structures can disrupt disturbances in the azimuthal direction. These observed reductions in correlation magnitudes could be incorporated into jet noise models to account for the presence of microjets.

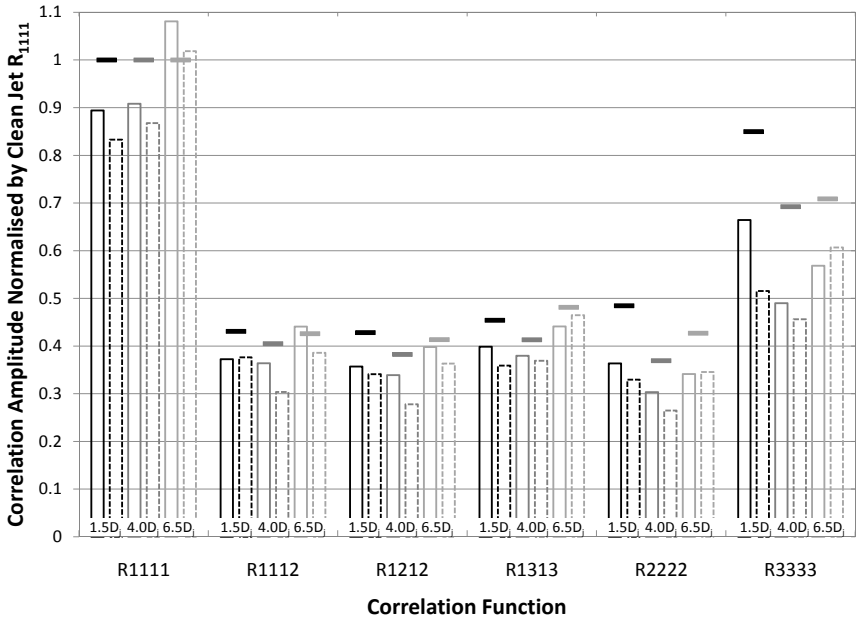

Figure 9: Relative amplitudes of fourth order correlations. Solid outline vertical bars: in line with the microjets; dashed outline vertical bars: between the microjets; solid horizontal bars: clean jet.

4. CONCLUSIONS

For this configuration of eight high pressure microjets acting upon a Mach 0.75 jet at a Reynolds number of 1 million, large eddy simulations show the microjets penetrate the shear layer producing streamwise vorticity on the inside of the jet. This dissipates before the end of the potential core and there is no effect on potential core length. The peak turbulence intensity within the shear layer is reduced, with the greatest reduction at locations aligned with the microjet injection points. The shapes of the fourth order correlation envelopes are little changed by the microjets, but there is a significant difference in the absolute magnitudes. Compared to a clean jet, all significant correlation terms are reduced, with the reduction still occurring at x/D_j=6.5 where the effect of the microjets on the mean flow has dissipated. This reduction could be used to calibrate a jet noise model in order to take account of the microjets.

ACKNOWLEDGEMENTS

The UK Turbulence Consortium under funding from the EPSRC grant EP/G069581/1 provided computing time for these calculations.

REFERENCES

[1] Alkislar, M.B., "Aeroacoustics of a Mach 0.9 Jet with Chevron-Microjet Combination," AIAA 2008-3041, 14th AIAA/CEAS Aeroacoustics Conference, Vancouver, Canada, 5-7 May 2008.

[2] Alkislar, M.B., Krothapalli, A., and Butler, G.W., The Effect of Streamwise Vortices on the Aeroacoustics of a Mach 0.9 Jet, Journal of Fluid Mechanics, Vol 578, pp 139–169, 2007.

[3] Bridges, J. and Brown, C.A., "Parametric Testing of Chevrons on Single Flow Hot Jets", AIAA 2004-2824, 10th Aeroa- coustics Conference, Manchester, UK, 10-12 May 2004.

[4] Castelain, T., Sunyach, M., Juve, D., and Bera, J.-C., Jet-Noise Reduction by Impinging Microjets: An Acoustic Inves- tigation Testing Microjet Parameters, AIAA Journal, Vol 46, pp 1081–1087, 2008.

[5] Aberg, M., Szasz, R.Z., Fuchs, L., and Gutmark, E., "Numerical Study of Fluidic Injection for Noise Reduction," AIAA 2007-11, 45th AIAA Aerospace Sciences Meeting and Exhibit, Reno, Nevada, 8-11 January 2007.

[6] Huet, M., Fayard, B., Rahier, G., and Vuillot, F., "Numerical Investigation of the Micro-Jets Efficiency for Jet Noise Reduction," AIAA 2009-3127, 15th AIAA/CEAS Aeroacoustics Conference, Miami, Florida, 11-13 May 2009.

[7] Lew, P.-T., Najafiyazdi, A., and Mongeau, L., "Unsteady Numerical Simulation of a Round Jet with Impinging Micro- jets for Noise Suppression," AIAA 2010-18, 48th AIAA Aerospace Sciences Meeting, Orlando, Florida, 4-7 January 2010.

[8] Liu, J., Kailasanath, K., Ramamurti, R., Munday, D., and Gutmark, E., "Large-Eddy Simulations of a Supersonic Jet with Fluidic Injection for Noise Reduction," AIAA 2010-4024, 16th AIAA/CEAS Aeroacoustics Conference, Stockholm, Sweden, 7-9 June 2010.

[9] Lighthill, M.J., "On Sound Generated Numerically II. Turbulence as a Source of Sound," Proc. Roy. Soc. Lond., 1954.

[10] Karabasov, S.A., Afsar, M.Z., Hynes, T.P., Dowling, A.P., McMullan, W.A., Pokora, C.D., Page, G.J., and McGuirk, J.J., Jet Noise: Acoustic Analogy Informed by Large Eddy Simulation, AIAA Journal, Vol 48, pp 1312–1325, 2010.

[11] McMullan, W.A., Pokora, C.D., Page, G.J., McGuirk, J.J., "Large Eddy Simulation of a High Reynolds Number Sub- sonic Turbulent Jet for Acoustic Source Capture," AIAA 2008-2974, 14th AIAA/CEAS Aeroacoustics Conference, Vancouver, Canada, 5-7 May 2008.

[12] Pokora, C.D., "Spatio-Temporal Correlations of Jets using High-Speed Particle Image Velocimetry", Ph.D. thesis, Loughborough University, 2009.

[13] Pokora, C.D., McGuirk, J.J., "Spatio-Temporal Turbulence Correlations using High-Speed PIV in an Axisymmetric Jet", AIAA 2008-3028, 14th AIAA/CEAS Aeroacoustics Conference, Vancouver, Canada, 5-7 May 2008.

[14] Jordan P, Gervais Y, Valire J-C, Foulon H. Final results from single point measurements. Project deliverable D3.4, JEAN EU 5th Framework Programme, G4RD-CT2000-00313, 2002